arXiv:1612.06728v1 [quant-ph] 20 Dec 2016

Atom-photon interactions at the speed of light

Giuseppe Calajó and Peter Rabl
Vienna Center for Quantum Science and Technology,
Atominstitut, TU Wien, Stadionallee 2, 1020 Vienna, Austria
(Dated: December 21, 2016)

We describe the coupling of moving atoms to a one dimensional photonic waveguide in the regime where the atomic velocities are comparable to the effective speed of light. Such conditions could be achieved, for example, in photonic crystals or coupled resonator arrays, where the maximal photonic group velocity is significantly reduced compared to free space. In this case the interplay between a velocity-induced directionality and the emergence of effective divergencies in the photonic density of states gives rise to a range of novel phenomena and non-perturbative effects in the emission of photons and the resulting dipole-dipole interactions between moving atoms. We show that apart from potential nanophotonic implementations, Rydberg atoms flying above a coupled array of superconducting microwave resonators provide a versatile platform for exploring this new regime of pseudo-relativistic atom-light interactions under accessible experimental conditions.

PACS numbers: 42.50.Pq, 42.50 Nn, 42.50.Ct

The radiation of charged particles moving close to the speed of light is a long-studied problem of classical electrodynamics [1] with practical relevance for accelerator physics or the development of intense X-ray sources [2]. In contrast, the coupling of neutral atoms and molecules to classical or quantized fields is usually investigated under opposite conditions, where particle velocities are low and mainly affect the emission and absorption of photons via a linear Doppler shift. This effect, however, is the basis for laser cooling [3] and successive atom trapping techniques [4], which enabled the study of strong light-matter interactions even at the single photon level [5–8]. Based on the same techniques, it has recently become possible to interface cold atoms with one dimensional (1D) waveguides [9, 10] and photonic crystal structures [11, 12], inside which the propagation velocity of photons can be significantly reduced [13]. This opens up new possibilities for exploring an intriguing regime of atom-light interactions, where individual atoms and photons move at comparable velocities, while still interacting strongly with each other.

The coupling of atoms or other emitters [14] to 1D waveguides, photonic crystals or coupled-cavity arrays has already attracted considerable attention. In this context, many interesting phenomena like single and multi-photon scattering [15–18], atom-photon bound states [1, 18–23, 25–27], self-organization [28, 29] and quantum many-body effects [30–32], or unidirectional emission [33–37] have been explored, usually under the assumption of stationary or slowly moving emitters. In this work we go beyond this conventional scenario and study atom-photon interactions in slow-light waveguides under conditions, where the atomic velocities approach, match or even exceed the effective speed of light. In particular, we show how a bounded group velocity introduces different types of directionalities and novel non-perturbative effects in photon emission and photon-transfer processes. We further describe a new realization of a slow-light waveguide QED system consisting of Rydberg atoms flying across a coupled array of planar microwave resonators [3, 8, 39–41]. This setting provides a versatile experimental platform for exploring such pseudo-relativistic light-matter interactions and study, for example, classical effects like Cherenkov radiation [43–46] in a quantum optical context, where each individual photon is interacting strongly with the moving atoms.

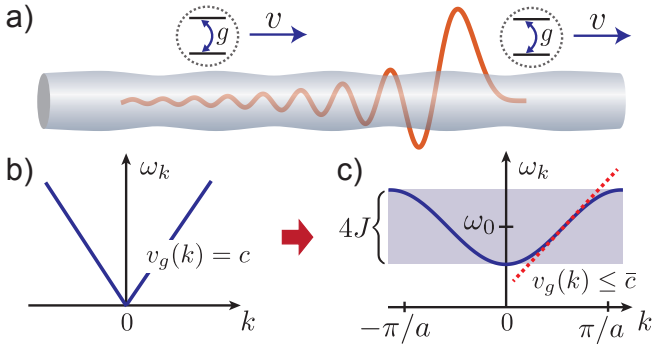

FIG. 1. Setup. a) Two-level atoms moving at a velocity v are strongly coupled to the evanescent field of a 1D waveguide. By introducing a sufficiently strong spatial modulation with periodicity a, photons are slowed down by Bragg-reflection and the usual linear dispersion relation shown in b) separates into individual bands of finite width $4J$, as indicated in c). Within one band the maximal group velocity is bounded by an effective speed of light, $\bar{c} = 2Ja$, which can be comparable to typical atomic velocities.

Model.—We consider a setup as shown in Fig. 1 a), where N two-level atoms are coupled to the field of a 1D photonic waveguide. The atoms have a mass m and the internal ground state $|g\rangle$ and excited state $|e\rangle$ are separated in frequency by ω_a. Restricted to the atomic motion along the waveguide direction, $\vec{e}_z$, the generic Hamil-

tonian for this system reads

$$H = \sum_{i=1}^{N}\left(\frac{p_i^2}{2m} + \hbar\omega_a|e\rangle_i\langle e|\right) + \int dk\,\hbar\omega_k\, a_k^\dagger a_k + \hbar\sum_{i=1}^{N}\int \frac{dk}{\sqrt{2\pi}}\left(g_k e^{ikz_i}a_k\sigma_+^i + g_k^* e^{-ikz_i}a_k^\dagger\sigma_-^i\right). \quad (1)$$

Here the z_i and p_i are the atomic position and momentum operators, $\sigma_-^i = (\sigma_+^i)^\dagger = |g\rangle_i\langle e|$, and the a_k, where $[a_k, a_{k'}] = \delta(k-k')$, are the bosonic annihilation operators for photons with wavevector k.

In conventional waveguides and within the relevant frequency range, $g_k \simeq g$ and $\omega_k \simeq (c/n)|k|$, where c is the speed of light in vacuum and $n \sim \mathcal{O}(1)$ is the refractive index of the material. Therefore, in this case the photonic group velocity, $v_g(k) = \partial\omega_k/\partial k \sim 10^8$ m/s, is much larger than typical atomic velocities, $v \lesssim 10^4$ m/s. To achieve a condition $v \sim v_g$, we consider in this work a waveguide with a spatially periodic modulation, for example, of its width, refractive index, etc. Provided that this modulation is sufficiently strong, the propagation of photons is slowed down by Bragg-reflection [13] and the spectrum separates into individual bands with an approximate dispersion relation $\omega_k \simeq \omega_0 - 2J\cos(ka)$, where a is the lattice constant and $4J$ is the total width of the band. This introduces an effective speed of light, $\bar{c} = \max\{v_g(k)\} = 2Ja$, corresponding to the maximal propagation velocity within the band. It can be tuned close to zero by taking the limiting case of a weakly tunnel-coupled array of individual resonators, making the regime $v \sim \bar{c}$ experimentally accessible.

It is important to keep in mind that by following this approach one changes from a continuum to a Bloch-wave description and introduces as well a periodic variation of the coupling, $g \to g(z)$. For atoms moving along classical trajectories $z_i(t) = z_i + v_i t$, this translates into a time-periodic modulation of the coupling and makes the dynamics of slow-light systems in general quite involved. However, for a large range of parameters, in particular for the relevant case of high velocities, $v \sim \bar{c}$, and ω_a within the propagation band, we can derive an effective model

$$H(t) \simeq \sum_{i=1}^{N}\hbar\omega_a|e\rangle_i\langle e| + \int_{-\frac{\pi}{a}}^{\frac{\pi}{a}} dk\,\hbar\omega_k a_k^\dagger a_k + \sum_{i=1}^{N}\sqrt{\frac{a}{2\pi}}\int_{-\frac{\pi}{a}}^{\frac{\pi}{a}} dk\,\hbar\bar{g}\left(e^{ikz_i(t)}a_k\sigma_+^i + e^{-ikz_i(t)}a_k^\dagger\sigma_-^i\right), \quad (2)$$

where only the coupling averaged over one unit cell, $\bar{g}$, appears. This model now mimics very closely the coupling of fast moving atoms to arbitrarily slow photons in a 1D continuum and will be used as a starting point for the following analysis. Details on the derivation of Eq. (2) and its range of validity are summarized in the supplementary material [47].

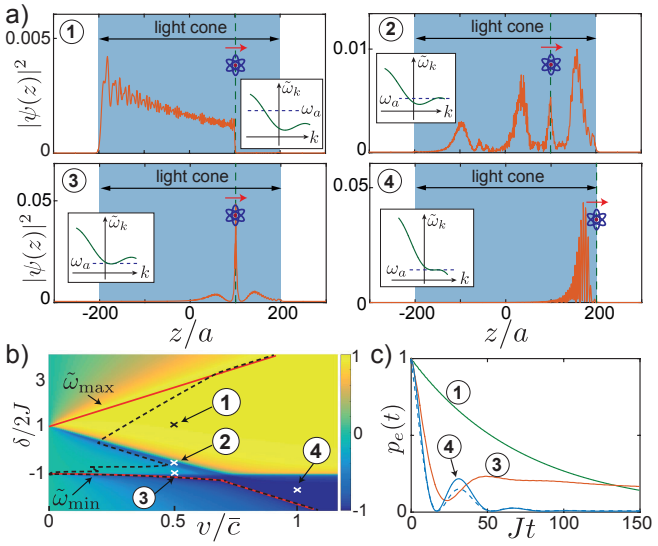

FIG. 2. a) Snapshots of the emitted photon wavepacket evaluated at a time $t = 100/J$ and for the parameters ① $v = \bar{c}/2$, $\delta/(2J) = 1$, ② $v = \bar{c}/2$, $\delta/(2J) = -0.5$, ③ $v = \bar{c}/2$, $\delta/(2J) = -1.1$ and ④ $v = \bar{c}$, $\delta/(2J) = -\pi/2$. The insets show the shape of the tilted dispersion relation, $\tilde{\omega}_k$, and the blue shaded area indicates the light cone, $|z| \leq \bar{c}t$. b) Plot of the directionality parameter D as function of δ and v. The solid red lines indicate the minimal and maximal frequency of the tilted band. For each detuning, the dashed line shows the minimal velocity $v_{\min}(\delta)$, above which the effective model (2) provides an accurate description of the dynamics [47]. c) Decay of the excited state population $p_e(t)$ for different sets of parameters. The dashed line indicates the approximate analytic solution given in Eq. (4) for $v = \bar{c}$ and $\delta/(2J) = -\pi/2$. In all plots a coupling of $\bar{g}/(2J) = 0.1$ is assumed.

Photon emission in the quasi-relativistic regime.—We first consider the emission of a photon from a single atom moving at a constant velocity $v > 0$. By assuming that at time $t = 0$ the atom is in state $|e\rangle$ and the waveguide in the vacuum state $|\text{vac}\rangle$, the state of the whole system can be written as $|\psi(t)\rangle = \left[c_e(t)\sigma_+ + \int dk\,\psi(k,t)a_k^\dagger\right]|g\rangle|\text{vac}\rangle$, where $p_e(t) = |c_e(t)|^2$ is the excited state population and $\psi(k,t)$ is the wavefunction of the emitted photon in k-space. Figure 2 a) shows snapshots of the resulting wavefunction in the discretized position space, $\psi(z,t)$, for different ratios $v/\bar{c}$ and different atom detunings $\delta = \omega_a - \omega_0$.

To obtain a better understanding of these emission patterns, it is convenient to change into a co-moving frame via the unitary transformation $\tilde{H} = UHU^\dagger + i\hbar\dot{U}U^\dagger$, where $U(t) = e^{i\sum_k vka_k^\dagger a_k t}$. In this new representation the time-dependence in the exponentials is eliminated, $z(t) \to z$, but we obtain instead a tilted dispersion relation $\omega_k \to \tilde{\omega}_k = \omega_k - kv$. For frequencies ω_a inside this tilted band and for sufficiently small $\bar{g}$, the coupling to

the waveguide will result in an approximately exponential decay of $p_e(t)$ with total rate $\Gamma = \Gamma_L + \Gamma_R$, where

$$\Gamma_{L,R} = \frac{\bar{g}^2 a}{|\tilde{v}_g(k_{L,R})|}. \tag{3}$$

Here $k_L < 0$ and $k_R > 0$ are left- and right-propagating wavevectors defined by the resonance condition $\tilde{\omega}_k = \omega_a$, and $\tilde{v}_g(k) = v_g(k) - v$ is the group velocity in the co-moving frame. In the usual case, where $v_g(k) \simeq \pm\bar{c}$ and $v \ll \bar{c}$, Eq. (3) implies that photons are emitted with Doppler-shifted wavevectors $k_{L,R} = \mp\omega_a/(\bar{c} \pm v)$, but with the same group velocity in the laboratory frame and approximately the same rates $\Gamma_L \simeq \Gamma_R$.

In the quasi-relativistic regime $v \sim \bar{c}$, this picture changes significantly. As illustrated in example ① in Fig. 2 a), the tilting of the finite propagation band opens a frequency window, within which only backward propagating modes exist. This gives rise to a purely unidirectional emission opposite to the atomic motion. A different mechanism for directionality is shown in example ②, where instead forward emission is enhanced near a divergence of the photonic density of states, i.e. $\tilde{v}_g(k_R) \simeq 0$, associated with the tilted right band edge. The combination of these effects can give rise to strong variations in the direction, the rate and the group velocity of the emitted photons as a function of the atomic velocity and detuning. This is summarized in Fig. 2 b), where we plot the directionality parameter $D = \frac{\Gamma_L - \Gamma_R}{\Gamma_L + \Gamma_R}$ [37, 48]. Note that for this plot we have assumed a finite decay rate $\gamma_p/J = 0.01$ for the photons, which allows us to generalize Eq. (3) to frequencies outside the band and to avoid unphysical divergencies [25].

The exponential decay with rates $\Gamma_{L,R}$ given in Eq. (3) assumes a perturbative treatment of the atom-light coupling, which is strictly valid only for $\bar{g} \to 0$. For static atoms it is well known that even for $\bar{g} \ll J$, the divergencies in the photonic density of states near the band-edges result in non-perturbative effects, like an oscillatory decay [21, 22] and the emergence of atom-photon bound states [20]. Examples ② and ③ in Fig. 2 a) show that such effects prevail even at very high velocities. A large fraction of the photon is coherently reabsorbed and remains bound to the moving atom for a long time. Note, however, that for moving atoms true bound states only exist within the effective continuum model (2). Zeros in the modulated coupling $g(z)$ in the full model will eventually lead to a complete decay of the atom [47].

Photon emission at the speed of light.—In addition to the above mentioned band edge effects, which are already present at low atomic velocities [46], a new and very unique situation occurs when the atomic velocity matches the speed of light, $v = \bar{c}$ (see example ④ in Fig. 2). In this case one obtains a cubic dispersion relation $\tilde{\omega}_k(k) \simeq -\pi J - \frac{Ja^3}{3}(k - k_c)^3$ for wavevectors around $k_c = \pi/(2a)$. This results in a higher order divergency

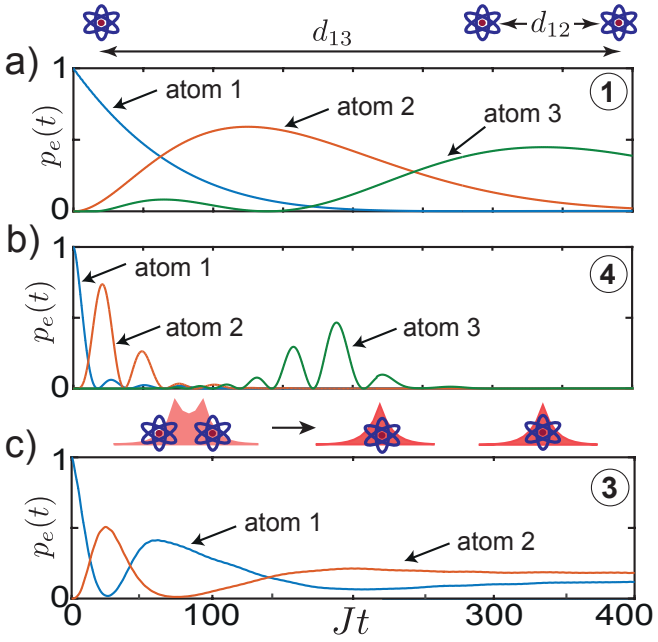

FIG. 3. Excitation transfer between moving atoms. In the first two plots three atoms moving with the same velocity $v > 0$ and relative separations $d_{12}/a = 2$ and $d_{13}/a = 45$ are considered. The parameters in a) are $v = \bar{c}/2$ and $\delta/(2J) = 1$ and in b) $v = \bar{c}$ and $\delta/(2J) = -\pi/2$. For the plot in c) two atoms with $z_1(0) = z_2(0)$, slightly different velocities $v_1 = 0.5\bar{c}$ and $v_2 = 0.53\bar{c}$ and a detuning of $\delta/(2J) = -1.1$ have been assumed. In all plots $\bar{g}/(2J) = 0.1$.

$\sim (\omega - \pi J)^{-2/3}$ in the effective photon density of states, as a consequence of the strong interactions between the moving atom and the co-propagating Cherenkov photon. However, in contrast to usual band-edge effects, this velocity-induced singularity lies in the middle of the band and for moderate $\bar{g}$ there is no bound state associated with it. As a result, the atom approximately decays as [47]

$$p_e(t) \simeq \cos^2(\Omega_c t) e^{-\Gamma_c t}, \tag{4}$$

where coherent atom-photon oscillations and decay occur with the same characteristic rate $\Omega_c \simeq 1.5\Gamma_c \simeq 0.6(\bar{g}^6/J)^{\frac{1}{5}}$. For a given $\bar{g} \ll J$, this is also the fastest rate at which the atom can be completely deexcited by emitting a highly localized photonic wave packet, which closely follows the atom in forward direction. At even higher velocities, $v > \bar{c}$, the density of states, and therefore also the emission rate, decreases again. As shown in Fig. 2 b), the directionality of the emitted photon is then only determined by the condition $\delta \lesseqgtr -2J$. For $\delta = -2J$ an extended photon, which is essentially stationary in the laboratory frame, is produced.

Excitation transfer processes.—Compared to conventional Cherenkov radiation studied in higher dimensional structures [44–46], a key feature of the current setting is that all emitted photons are confined to one dimen-

sion and can thus be efficiently reabsorbed by other atoms. For conventional waveguides, this emission and reabsorption of photons gives rise to almost instantaneous, long-range and bidirectional dipole-dipole interactions, which depend only on the relative atomic positions, $|z_i - z_j|$ [49, 50]. In the quasi-relativistic regime various qualitatively different excitation transfer processes arise, depending strongly on the velocities and detunings of the involved atoms. To illustrate this point we first consider in Fig. 3 a) and b) the case of three atoms moving at the same speed $v > 0$, with the first atom to the right being initially prepared in the excited state. At rest the maximal population transfer to atoms 2 and 3 would be limited by the fraction of population trapped in the sub-radiant state [51–53], and $p_e^{(2,3)}(t) < 0.25$. This limit no longer applies at moderate and fast velocities, where the emission becomes highly directional and therefore also results in a much more efficient transfer of excitations from the right to the left. Note that for the parameters assumed in Fig. 3 a), the retardation time $\tau_{13} = |d_{13}/(v_g(k_L) - v)|$ is still short compared to the timescale of the transfer dynamics ($\sim \Gamma_L^{-1}$) and the whole process is well described by a unidirectional markovian master equation [36] in the co-moving frame. This is no longer the case for the critical condition $v = \bar{c}$ and $\delta/J = -\pi$ assumed in Fig. 3 b). Here we observe a very rapid transfer of the initial excitation from atom 1 to atom 2, which is mediated by the highly compressed Cherenkov photon shown in example ④ in Fig. 2 a). This photon then slowly falls behind and at a much later time overlaps with atom 3. The resulting oscillation between the photon and atom 3 with roughly the same Rabi frequency Ω_c as identified in Eq. (4), are again a clear signature of the highly non-markovian nature of the transfer process.

Finally, in Fig. 3 c) we consider another example, where two initially co-propagating atoms exchange excitations via a co-moving bound photon, which remains exponentially localized around the atomic positions $z_i(t)$. By introducing a small velocity difference, i.e. $v_1 \neq v_2$, the atoms slowly separate and gradually decouple. Depending on the detailed choice of parameters, the photon may remain with one of the atoms or be split into two separated atom-photon bound states [25].

Implementation.—While the approach for realizing the slow-light Hamiltonian (2) is very generic and could potentially be implemented with optimized nanophotonic crystal structures, the conditions for reaching the pseudo-relativistic regime are still very challenging. In particular, local disorder must be small compared to $4J$ to avoid photon localization [47, 54], and fast moving atoms must be guided very close to the surface such that the emission into the waveguide exceeds the remaining decay into free space. To overcome these problems we propose here an equivalent system in the microwave regime, where Rydberg atoms [3, 39–41] fly above a coupled array of superconducting transmission line resonators, as shown Fig. 4 a). The resonators of length $L_x \sim 1$ cm exhibit standing wave modes with frequencies $\omega_0 = c\pi/L_x$ in the GHz regime, while in z-direction the electric field is strongly confined to a few tens of μm determined by the size of the middle electrode, $2l_1$ [see Fig. 4 b)]. By considering an array of parallel resonators separated by $a \approx 200\,\mu$m, we obtain a closely spaced resonator array with a tunnel coupling J that can be fully adjusted by additional capacitive couplings at the end-points [8, 27].

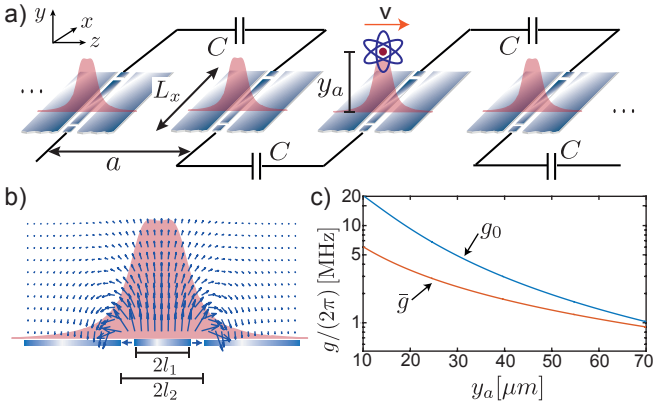

FIG. 4. Slow-light waveguide QED with Rydberg atoms. a) Rydberg atoms fly at a distance y_a above an array of parallel CPW resonators coupled by capacitances C. b) Cross section of a single resonator and sketch of the transverse field distribution. c) Atom-field coupling strength as a function of the atom-surface distance y_a for the example described in the text. Here g_0 denotes the maximal coupling evaluated at $z = 0$ and $\bar{g}$ the corresponding average coupling, which is used in the effective continuum model (2). See Ref. [47] for more details.

As a specific example, we consider a microwave resonator with dimensions $L_x = 0.5$ cm, $l_1 = 10\,\mu$m, $l_2 = 15\,\mu$m and $\omega_0/(2\pi) \approx 30$ GHz. By identifying two Rydberg states with neighboring principle quantum numbers n, i.e. $|g\rangle = |n\rangle$ and $|e\rangle = |n+1\rangle$, we obtain a resonant coupling $\omega_a = \omega_{n+1} - \omega_n \simeq \omega_0$ for $n \simeq 50$. The resulting maximal atom-field coupling $g_0 = d_{n,n+1}E_0(y_a)/\hbar$ [3, 39], where $d_{n,n+1}$ is the transition dipole moment and $E_0(y_a)$ the electric field per photon, as well as the corresponding averaged coupling, $\bar{g}$, are plotted in Fig. 4 c) as a function of the atom surface distance, y_a. For an atomic beam of velocity $v = 10^4$ m/s [39] we choose a capacitive coupling $J/(2\pi) = 4$ MHz to obtain $v/\bar{c} \approx 1$ and still being larger than the typical level of on-site disorder [8]. Therefore, already at convenient distances of $y_a \approx 50\,\mu$m we obtain $\bar{g} \sim J$ and for the validity of the effective model we can chose a smaller value of $\bar{g}/J \simeq 0.1$, by adjusting the position of the beam along the x-direction. On the relevant timescale set by $\Gamma_c/(2\pi) \approx 400$ kHz, both the decay rate of the Rydberg states, $\gamma_a/(2\pi) \simeq 1$ kHz, and the photon loss rate $\gamma_p/(2\pi) \simeq 30$ kHz of a high-Q microwave resonator [55] are still negligible. Note that

for an array of ~ 500 resonators with a total length of $L = 10$ cm, the condition on the transverse spread during the flight time, $\Delta y/y_a < 1$, requires a transverse cooling of the atom beam to a few mK, or alternatively, on-chip guiding systems for Rydberg atoms [56]. This shows that microwave-based slow-light systems are well within reach of existing experimental capabilities.

Conclusions.—In summary, we have described atom-photon interactions in the pseudo-relativistic regime, where the atomic velocities are comparable to the maximal speed of light in a waveguide structure. Under such conditions the atomic motion drastically changes photon emission and transfer processes and induces a strong directionality and novel non-perturbative effects. Importantly, we have shown that Rydberg atoms flying above a coupled array of microwave resonator provide a versatile platform, where this combination of quasi-relativistic and strong-coupling quantum optical effects is experimentally accessible.

Acknowledgments.—The authors thank D. Chang, P. Schneeweiss, J. Volz, A. Rauschenbeutel and F. Ciccarello for valuable feedback. This work was supported by the Austrian Science Fund (FWF) through SFB FOQUS F40, DK CoQuS W 1210 and the START grant Y 591-N16.

[1] J. D. Jackson, *Classical electrodynamics* (John Wiley & Sons, 1962).

[2] Z. Huang and K. J. Kim, *Review of x-ray free-electron laser theory*, Phys. Rev. ST Accel. Beams **10**, 034801 (2007).

[3] S. Stenholm, *The semiclassical theory of laser cooling*, Rev. Mod. Phys. **58**, 699 (1986).

[4] H. J. Metcalf and P. van der Straten, *Laser Cooling and Trapping* (Springer, 1999).

[5] K. M. Birnbaum, A. Boca, R. Miller, A. D. Boozer, T. E. Northup, and H. J. Kimble, *Photon blockade in an optical cavity with one trapped atom*, Nature (London) **436**, 87 (2005).

[6] T. G. Tiecke, J. D. Thompson, N. P. de Leon, L. R. Liu, V. Vuletic, and M. D. Lukin, *Nanophotonic quantum phase switch with a single atom*, Nature (London) **508**, 241 (2014).

[7] J. Volz, M. Scheucher, C. Junge, and A. Rauschenbeutel, *Nonlinear π phase shift for single fibre-guided photons interacting with a single resonator-enhanced atom*, Nat. Photon. **8**, 965 (2014).

[8] B. Hacker, S. Welte, G. Rempe, and S. Ritter, *A photon-photon quantum gate based on a single atom in an optical resonator*, Nature (London) **536**, 193 (2016).

[9] D. Reitz, C. Sayrin, R. Mitsch, P. Schneeweiss, and A. Rauschenbeutel, *Coherence Properties of Nanofiber-Trapped Cesium Atoms*, Phys. Rev. Lett. **110**, 243603 (2013).

[10] R. Yalla, M. Sadgrove, K. P. Nayak and K. Hakuta, *Cavity Quantum Electrodynamics on a Nanofiber Using a Composite Photonic Crystal Cavity*, Phys. Rev. Lett. **113**, 143601 (2014).

[11] J. D. Thompson, T. G. Tiecke, N. P. de Leon, J. Feist, A. V. Akimov, M. Gullans, A. S. Zibrov, V. Vuletic, and M. D. Lukin, *Coupling a single trapped atom to a nanoscale optical cavity*, Science **340**, 1202 (2013).

[12] A. Goban, C.-L. Hung, S. P. Yu, J. D. Hood, J. A. Muniz, J. H. Lee, M. J. Martin, A. C. McClung, K. S. Choi, D. E. Chang, O. Painter, and H. J. Kimble, *Atom-light interactions in photonic crystals*, Nat. Commun. **5**, 3808 (2014).

[13] T. F. Krauss, *Slow light in photonic crystal waveguides*, J. Phys. D: Appl. Phys. **40**, 2666 (2007).

[14] P. Lodahl, S. Mahmoodian, and S. Stobbe, *Interfacing single photons and single quantum dots with photonic nanostructures*, Rev. Mod. Phys. **87**, 347 (2015).

[15] J. T. Shen and S. Fan, *Strongly Correlated Two-Photon Transport in a One-Dimensional Waveguide Coupled to a Two-Level System*, Phys. Rev. Lett. **98**, 153003 (2007).

[16] L. Zhou, Z. R. Gong, Y. X. Liu, C. P. Sun, and F. Nori, *Controllable Scattering of a Single Photon inside a One-Dimensional Resonator Waveguide*, Phys. Rev. Lett. **101**, 100501 (2008).

[17] T. Shi and C. P. Sun, *Lehmann-Symanzik-Zimmermann reduction approach to multiphoton scattering in coupled-resonator arrays*, Phys. Rev. B **79**, 205111 (2009).

[18] P. Longo, P. Schmitteckert, and K. Busch, *Few-Photon Transport in Low-Dimensional Systems: Interaction-Induced Radiation Trapping*, Phys. Rev. Lett. **104**, 023602 (2010).

[19] P. Bykov, *Spontaneous emission from a medium with a band spectrum*, Sov. J. Quant. Electron. **4**, 7 (1975).

[20] S. John and J. Wang, *Quantum electrodynamics near a photonic band gap: Photon bound states and dressed atoms*, Phys. Rev. Lett. **64**, 2418 (1990).

[21] S. John and T. Quang, *Spontaneous emission near the edge of a photonic band gap*, Phys. Rev. A **50**, 1764 (1994).

[22] A. G. Kofman, G. Kurizki, and B. Sherman, *Spontaneous and induced atomic decay in photonic band structures*, J. Mod. Opt. **41**, 353 (1994).

[23] P. Lambropoulos, G. M. Nikolopoulos, T. R. Nielsen, and S. Bay, *Fundamental quantum optics in structured reservoirs*, Rep. Prog. Phys. **63**, 455 (2000).

[24] F. Lombardo, F. Ciccarello, and G. M. Palma, *Photon localization versus population trapping in a coupled-cavity array*, Phys. Rev. A **89**, 053826 (2014).

[25] G. Calajo, F. Ciccarello, D. Chang and P. Rabl, *Atom-field dressed states in slow-light waveguide QED*, Phys. Rev. A **93**, 033833 (2016).

[26] T. Shi, Y-H. Wu, A. Gonzalez-Tudela and J. I. Cirac, *Bound States in Boson Impurity Models*, Phys. Rev. X **6**, 021027 (2016).

[27] Y. Liu and A. Houck, *Quantum electrodynamics near a photonic bandgap*, Nature Phys. (2016); doi:10.1038/nphys3834.

[28] D. E. Chang, J. I. Cirac, and H. J. Kimble, *Self-Organization of Atoms along a Nanophotonic Waveguide*, Phys. Rev. Lett. **110**, 113606 (2013).

[29] T. Grießer and H. Ritsch, *Light-Induced Crystallization of Cold Atoms in a 1D Optical Trap*, Phys. Rev. Lett. **111**, 055702 (2013).

[30] M. J. Hartmann, F. G. S. L. Brandão and M. B. Plenio, *Strongly interacting polaritons in coupled arrays of cavities*, Nature Phys. **2**, 849 (2006).

[31] A. D. Greentree, C. Tahan, J. H. Cole, and C. L. Hollenberg, *Quantum phase transitions of light*, Nature Phys. **2**,

856 (2006).
[32] D. G. Angelakis, M. F. Santos, and S. Bose, *Photon-blockade-induced Mott transitions and XY spin models in coupled cavity arrays*, Phys. Rev. A **76**, 031805(R) (2007).
[33] J. Petersen, J. Volz, and A. Rauschenbeutel, *Chiral nanophotonic waveguide interface based on spin-orbit interaction of light*, Science **346**, 67 (2014).
[34] R. Mitsch, C. Sayrin, B. Albrecht, P. Schneeweiss, and A. Rauschenbeutel, *Quantum state-controlled directional spontaneous emission of photons into a nanophotonic waveguide*, Nat. Commun. **5**, 5713 (2014).
[35] I. Söllner, *et al.*, *Deterministic photon-emitter coupling in chiral photonic circuits*, Nature Nanotech. **10**, 775 (2015).
[36] K. Stannigel, P. Rabl and P. Zoller, *Driven-dissipative preparation of entangled states in cascaded quantum-optical networks*, New J. Phys. **14**, 063014 (2012).
[37] P. Lodahl, S. Mahmoodian, S. Stobbe, P. Schneeweiss, J. Volz, A. Rauschenbeutel, H. Pichler, P. Zoller, *Chiral Quantum Optics*, arXiv:1608.00446 (2016).
[38] D. Petrosyan and M. Fleischhauer, *Quantum Information Processing with Single Photons and Atomic Ensembles in Microwave Coplanar Waveguide Resonators*, Phys. Rev. Lett. **100**, 170501 (2008).
[39] S. D. Hogan, J. A. Agner, F. Merkt, T. Thiele, S. Filipp, and A. Wallraff, *Driving Rydberg-Rydberg Transitions from a Coplanar Microwave Waveguide*, Phys. Rev. Lett. **108**, 063004 (2012).
[40] C. Hermann-Avigliano, R. Celistrino Teixeira, T. L. Nguyen, T. Cantat-Moltrecht, G. Nogues, I. Dotsenko, S. Gleyzes, J. M. Raimond, S. Haroche, and M. Brune, *Long coherence times for Rydberg qubits on a superconducting atom chip*, Phys. Rev. A **90**, 040502(R) (2014).
[41] M. A. Beck, J. A. Isaacs, D. Booth, J. D. Pritchard, M. Saffman, R. McDermott, *Optimized Coplanar Waveguide Resonators for a Superconductor-Atom Interface*, Appl. Phys. Lett. **109**, 092602 (2016).
[42] D. Underwood, W. E. Shanks, J. Koch, and A. A. Houck, *Low disorder microwave cavity lattices for quantum simulation with photons*, Phys. Rev. A **86**, 023837 (2012).
[43] P. A. Cherenkov, *Visible Radiation Produced by Electrons Moving in a Medium with Velocities Exceeding that of Light*, Dokl. Akad. Nauk **2**, 451 (1934) [Phys. Rev. **52**, 378 (1937)].
[44] J. V. Jelly, *Cerenkov Radiation and its Applications* (Pergamon, London, 1958).
[45] C. Luo, M. Ibanescu, S. G. Johnson, J. D. Joannopoulos, *Cerenkov Radiation in Photonic Crystals*, Science **299**, 5605 (2003).
[46] C. Luo, M. Ibanescu, E. J. Reed, S. G. Johnson, J. D. Joannopoulos, *Doppler Radiation Emitted by an Oscillating Dipole Moving inside a Photonic Band-Gap Crystal*, Phys. Rev. Lett. **96**, 043903 (2006).
[47] See the supplemental material for more detailed derivations of the main results presented.
[48] C. Gonzalez-Ballestero, E. Moreno, F.J. Vidal, A. Gonzalez-Tudela, *Non-reciprocal few-photon devices based on chiral waveguide-emitter couplings*, Phys. Rev. A 94, **94**, 063817 (2016).
[49] D. E. Chang, L. Jiang, A. V. Gorshkov, and H. J. Kimble, *Cavity QED with atomic mirrors*, New J. Phys. **14**, 063003 (2012).
[50] A. González-Tudela and D. Porras, *Mesoscopic Entanglement Induced by Spontaneous Emission in Solid-State Quantum Optics*, Phys. Rev. Lett. **110**, 080502 (2013).
[51] C. Gonzalez-Ballestero, F. J. Garcia-Vidal and E. Moreno, *Non-Markovian effects in waveguide-mediated entanglement*, New J. Phys. **15**, 073015 (2013).
[52] S. Longhi, *Bound states in the continuum in a single-level Fano-Anderson model*, Eur. Phys. J. B **57**, 45 (2007).
[53] P. Facchi, M. S. Kim, S. Pascazio, F. V. Pepe, D. Pomarico and T. Tufarelli, *Bound states and entanglement generation in waveguide quantum electrodynamics*, Phys. Rev. A **94**, 043839 (2016).
[54] J. C. Hernández-Herrejón, F. M. Izrailev and L. Tessieri, *Anomalous localization in the aperiodic Kronig-Penney model* Journal of Physics A: Mathematical and Theoretical **43**, 425004 (2010).
[55] L. Frunzio, A. Wallraff, D. Schuster, J. Majer, and R. Schoelkopf, IEEE Trans. Appl. Supercond. **15**, 860 (2005).
[56] P. Lancuba and S. D. Hogan, *Electrostatic trapping and in situ detection of Rydberg atoms above chip-based transmission lines*, J. Phys. B: At. Mol. Opt. Phys. **49**, 074006 (2016).

Supplemental material for: Atom-photon interactions at the speed of light

This supplemental material contains additional details on the model and the derivation of various results stated in the main part of the paper.

I. DERIVATION AND VALIDITY OF THE EFFECTIVE CONTINUUM MODEL

In this section we discuss in more detail the derivation and the validity of the effective continuum model given in Eq. (2) in the main text. For this analysis we assume that the motion of atoms is described by classical trajectories $z_i(t) = z_i + v_i t$, which is well justified for the parameter regime considered in this work. Under this assumption the kinetic term appearing in Eq. (1) in the main text is constant and the dynamics of the atoms can be reduced to their internal degrees of freedom.

To achieve slow-light conditions we consider a periodically modulated waveguide with lattice constant a and total length $L \gg a$. The Hamiltonian describing the coupling of the two-level atoms and the 1D field in the waveguide can then be written in the general form ($\hbar = 1$)

$$H(t) = \sum_{i=1}^{N} \omega_a |e\rangle_i\langle e| + \sum_{k,b} \omega_{k,b}\, a^\dagger_{k,b} a_{k,b} + \sum_{i=1}^{N} g\left[F(z_i(t))\sigma^i_+ + F^\dagger(z_i(t))\sigma^i_-\right]. \tag{S1}$$

By assuming periodic boundary conditions the field operator is given by

$$F(z) = \sum_{k,b} \psi_{k,b}(z) a_{k,b}, \tag{S2}$$

where $a_{k,b}$ are bosonic annihilation operators obeying $[a_{k,b}, a^\dagger_{k',b'}] = \delta_{bb'}\delta_{kk'}$ and

$$\psi_{k,b}(z) = \sqrt{\frac{a}{L}} u_{k,b}(z) e^{ikz} \tag{S3}$$

are Bloch waves with band index b and wavevector $k \in (-\pi/a, \pi/a]$, $\Delta k = 2\pi/L$. The $u_{k,b}(z) = u_{k,b}(z+a)$ are periodic functions.

The slow-light limit that we are interested in corresponds to the tight-binding limit in electronic band structures. In this limit the frequency separation between neighboring bands, $\omega_{k,b+1} - \omega_{k,b} \sim c/a$, is much bigger than the variation of frequencies within one band. In this limit the dispersion relation of a single band can be approximated by $\omega_{k,b} \simeq \omega_0^b - 2J_b \cos(ka)$. By assuming in addition that also all the relevant frequency scales of the system dynamics (see below) are small compared to c/a, we can restrict our analysis to a single band with $\omega_0^b \approx \omega_a$. By omitting the band index we then obtain the single band model

$$H(t) \simeq \sum_{i=1}^{N} \omega_a |e\rangle_i\langle e| + \sum_k \omega_k\, a^\dagger_k a_k + \sum_{i=1}^{N} \sqrt{\frac{a}{L}} \sum_k \left(g_k(z_i(t)) e^{ikz_i(t)} a_k \sigma^i_+ + g^*_k(z_i(t)) e^{-ikz_i(t)} a^\dagger_k \sigma^i_- \right), \tag{S4}$$

where $g_k(z) = g u_k(z)$. Note that compared to the main text, we have considered here a system with a large, but finite number of lattice sites $N_L = L/a$ and g is given in units of frequency. Therefore, Eq. (S4) can be directly used for numerical simulations. The limit $L \to \infty$ can be obtained in the usual way by replacing $\sum_k \to L/(2\pi)\int_{-\pi/a}^{\pi/a} dk$ and $a_k \to \sqrt{2\pi/L}\, a_k$.

A. Continuum approximation

Due to their motion with constant velocity v_i, the atoms induce a time periodic modulation of the coupling with frequency $\Omega_i = 2\pi|v_i|/a$. This modulation makes the dynamics of moving atoms coupled to slow-light waveguides in general quite involved. To obtain a simpler description, which mimics closely the coupling of moving atoms to photons in a continuous waveguide, we focus in this work primarily on the case of very fast atoms where $\Omega_i \gg g$. In this

regime the modulation is fast compared to the interaction timescale g and we can replace the modulated couplings $g(z_i(t))$ by the coupling $\bar{g}$ averaged over one period, $T_i = 2\pi/\Omega_i$.

To be more precise, let us assume that at time $t = 0$ the i-th atom is located at the left border of one of the unit cells, i.e., $z_i(0) \equiv z_i = (n_1 - 1/2)a$, and the atom then traverses ℓ lattice sites. In the interaction picture with respect to the bare atom and photon Hamiltonian, the integrated coupling between the atom and a photonic mode a_k is then given by

$$G_k^\ell := \int_0^{\ell T_i} dt'\, g_k(z_i(t'))e^{ikz_i(t')}e^{i\delta_k t'} = \frac{g}{v_i}\int_{z_i}^{z_i+\ell a} dz\, u_k(z)e^{ikz}e^{i\delta_k(z-z_i)/v_i}, \tag{S5}$$

where $\delta_k = \omega_a - \omega_k$. We now use the fact that in the tight-binding limit,

$$u_k(z) \simeq \bar{u}(z)e^{-ikz} \qquad \text{for} \quad -a/2 < z < a/2, \tag{S6}$$

where $\bar{u}(z)$ is an approximately k-independent mode functions of one unit cell. Then,

$$G_k^\ell = gT_i\left[\frac{1}{a}\int_{-a/2}^{a/2} dz\, \bar{u}(z)e^{i\delta_k z/v_i}\right] \times \sum_{n=n_1}^{n_1+\ell-1} e^{ikan}e^{i\delta_k T_i(n+1/2)}. \tag{S7}$$

To proceed we neglect the variation $\sim e^{i\delta_k z/v_i}$ in the integral in Eq. (S7). This is valid for small detunings, $\delta_k \ll \Omega_i$, but also for strongly peaked $\bar{u}(z)$. Under this approximation we can introduce the average coupling

$$\bar{g} = g \times \frac{1}{a}\int_0^a dz\, \bar{u}(z), \tag{S8}$$

and obtain

$$G_k^\ell \simeq \bar{g}T_i \times \sum_{n=n_1}^{n_1+\ell-1} e^{ikan}e^{i\delta_k T_i(n+1/2)}. \tag{S9}$$

We see that this result is just the discretized version of the integral

$$G_k^\ell \simeq \bar{g}\int_0^{\ell T_i} dt'\, e^{ikz_i(t')}e^{i\delta_k t'}, \tag{S10}$$

which we would obtain for the same quantity evaluated for the continuum model

$$H(t) \simeq \sum_{i=1}^N \omega_a|e\rangle_i\langle e| + \sum_k \omega_k\, a_k^\dagger a_k + \sum_{i=1}^N \sqrt{\frac{a}{L}}\sum_k \bar{g}\left(e^{ikz_i(t)}a_k\sigma_+^i + e^{-ikz_i(t)}a_k^\dagger\sigma_-^i\right), \tag{S11}$$

which is just the finite-length version of the effective model given in Eq. (2) in the main text. Although in the derivation of Eq. (S11) several crude approximations have been involved, a numerical comparison with the full model given in Eq. (S4) shows that for all the parameters considered in this work very accurate qualitative and quantitative predictions with errors on the percent level can be obtained. However, as we discuss in the following, there are also regimes, where such an effective description breaks down.

B. Validity of the continuum approximation

Let us now discuss in more detail the range of validity for the continuum description. To do so we consider the evolution of a state in the single excitation subspace, which we write as $|\psi(t)\rangle = \left[\sum_i c_e^i(t)\sigma_+^i + \sum_k\, \psi(k,t)a_k^\dagger\right]|g\rangle|\text{vac}\rangle$. In the interaction picture with respect to $H_0 = \sum_{i=1}^N \omega_a|e\rangle_i\langle e| + \sum_k \omega_k\, a_k^\dagger a_k$ we obtain the following set of equations of motion

$$\begin{aligned}
\frac{dc_e^i(t)}{dt} &= -ig\sqrt{\frac{a}{L}}\sum_k \psi(k,t)u_{ki}(t)e^{i\tilde{\delta}_k^i t}e^{ikz_i},\\
\frac{d\psi(k,t)}{dt} &= -ig\sqrt{\frac{a}{L}}\sum_j c_e^j(t)u_{kj}^*(t)e^{-i\tilde{\delta}_k^j t}e^{-ikz_j},
\end{aligned} \tag{S12}$$

where $\tilde{\delta}_k^i = \omega_a - (\omega_k - v_i k)$ is the detuning of the atoms from the tilted band and $u_{ki}(t) \equiv u_k(z_i(t))$. After inserting the second equation into the first we obtain the following integro-differential equation

$$\frac{dc_e^i(t)}{dt} = -\frac{g^2 a}{L} \sum_j \sum_k e^{ik(z_i - z_j)} u_{ki}(t) e^{i\tilde{\delta}_k^i t} \int_0^t dt' u_{kj}^*(t') e^{-i\tilde{\delta}_k^j t'} c_e^j(t'). \tag{S13}$$

The $u_{ki}(t)$ are periodic in time with period $T_i = |v_i|/a$ and can be expanded in a Fourier series $u_{ki}(t) = \sum_n u_{ki}^n e^{i\Omega_i n t}$. The resulting expression can be written as

$$\begin{aligned} \frac{dc_e^i(t)}{dt} &= -\frac{g^2 a}{L} \sum_j \sum_{n,m} \sum_k u_{ki}^n [u_{kj}^m]^* e^{ik(z_i - z_j)} e^{i(\tilde{\delta}_k^i - \tilde{\delta}_k^j)t} e^{i(\Omega_i n - \Omega_j m)t} \int_0^t dt' e^{i\tilde{\delta}_k^j (t-t')} e^{i\Omega_j m (t-t')} c_e^j(t') \\ &= -\frac{g^2 a}{L} \sum_j \sum_k u_{ki}^0 [u_{kj}^0]^* e^{ik(z_i - z_j)} e^{i(\tilde{\delta}_k^i - \tilde{\delta}_k^j)t} \int_0^t dt' e^{i\tilde{\delta}_k^j (t-t')} c_e^j(t') \ + \text{ Rest.} \end{aligned} \tag{S14}$$

When evaluated under the same stroboscopic approximation as above, the first term in the second line of this equation simply corresponds to the evolution under the effective continuum model given in Eq. (S11). A first set of corrections arises from terms with $n \neq 0$, but $m = 0$. Such terms lead to additional oscillating contributions to $c_e^i(t)$. However, as long as $g \ll \Omega_i$, these corrections remain small and do not affect the long time behavior of $c_e^i(t)$.

More crucial are terms with $n = m \neq 0$, which can generate non-oscillating contributions that affect the slowly varying dynamics of $c_e^i(t)$. To see this more explicitly let us consider a single atom and a specific correction term

$$\begin{aligned} \left.\frac{dc_e(t)}{dt}\right|_{n=m} &= -\frac{g^2 a}{L} \sum_k |u_k^n|^2 \int_0^t dt' e^{i\tilde{\delta}_k (t-t')} e^{i\Omega n (t-t')} c_e(t') \\ &\approx -\left[\frac{\pi g^2 a}{L} \sum_k |u_k^n|^2 \delta\left(\tilde{\delta}_k^i + \Omega_i n\right)\right] c_e(t), \end{aligned} \tag{S15}$$

where in the second line we have made a Markov approximation and replaced the integral over t by a δ-function in frequency. From this estimate we see that the higher order correction terms can contribute additional decay channels with rates $\Gamma^{(n)}$ proportional to the density of states evaluated at the modulated frequency $\tilde{\delta}_k + n\Omega$. To ensure that such corrections do not affect the dynamics, all the frequencies $\omega_a + n\Omega_i$ must lie outside the tilted propagation band, as illustrated in Fig. S1 b). This condition can be recast into the form

$$\Omega_i = \frac{2\pi |v_i|}{a} > \max_k \left| \frac{\delta + 2J\cos ka}{1 - \frac{ak}{2\pi}} \right|, \tag{S16}$$

where $\delta = \omega_a - \omega_0$. The boundary derived from this inequality is represented by the blue line in Fig. S1 a).

It turns out that under certain conditions Eq. (S16) is too strict and the continuum model can be applied even at lower velocities. This is the case for ω_a tuned close to the lower band edge. As shown in Fig. S1 c), in this case the Ω sideband can lie within the propagation band, but since the density of states near the band edge is much higher, the resulting correction is still negligible compared to effective evolution. This explains why quasi-bound states near the lower band edge can be observed at finite velocities. However, since $\Gamma^{(1)}$ is non-zero, these bound states still decay on longer timescales.

C. Numerical verification

To verify the validity of our analytic estimates we can compare the predictions from the effective model (S11) with a numerical simulation of the full model (S4), which accounts for the exact time-dependence of the couplings. For these numerical simulations we consider the specific example, where the local mode at each lattice site is represented by a Gaussian wavepacket

$$\bar{u}(z) = \frac{1}{\pi^{1/4}} \sqrt{\frac{a}{z_0}} e^{-\frac{z^2}{2z_0^2}} \tag{S17}$$

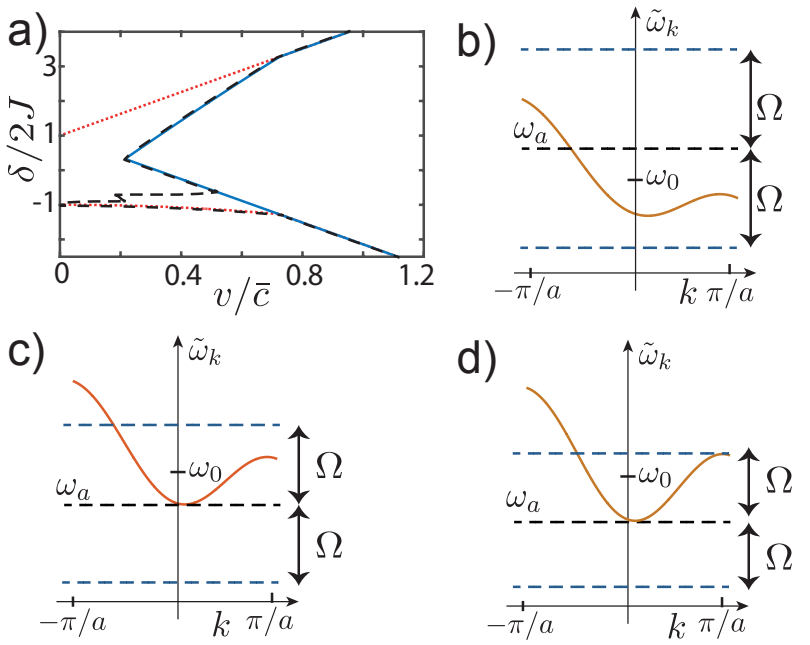

FIG. S1. a) Validity of the effective continuum model in the area spanned by δ and v. The blue continuous line shows the boundary derived from condition (S16), while the black dashed line represents the boundary derived from numerical simulations. On the right hand side of this line the predictions for $p_e(t)$ obtained from the full model (S4) and the effective model (S11) agree better than 10%. See text for more details. The dotted red lines indicte the lower and the upper edge of the tilted dispersion relation $\tilde{\omega}_k$. b)-d) Illustration of the higher order resonances shifted by $\pm\Omega$ for b) $v/\bar{c} = 0.5$ and $\delta/(2J) = 1$, c) $v/\bar{c} = 0.3$ and $\delta/(2J) = -1.05$ and d) $v/\bar{c} = 0.22$ and $\delta/(2J) = -1$.

with a width $z_0 \ll a$. This results in an average coupling

$$\bar{g} \simeq g\sqrt{\frac{2z_0}{a}}\pi^{1/4}. \tag{S18}$$

For the simulation of the full model we assume $g/(2J) = 0.1$ and $z_0/a = 0.1$. This corresponds to $\bar{g}/(2J) \simeq 0.06$.

By using the parameters given above we compare in Fig. S2 the predictions of the effective model and the full model for some of the values of δ and v assumed in Fig. (2) and Fig. (3) in the main text. For all the cases we see an excellent agreement between the exact and the effective evolution, in particular for the evolution of $p_e(t)$. Further, to verify the validity condition given in Eq. (S16) above, we evaluate the evolution for the excited state probability $p_e(t)$ up to a final time $T_f = 50/J$ for a wide range of parameters δ and v. Then, the discrepancy parameter

$$d = \max\{|p_e^{\text{eff}}(t) - p_e^{\text{full}}(t)|, 0 < t < T_f\}, \tag{S19}$$

can be used to quantify the validity of the effective model. In Fig. S1 a) we plot the boundary set by $d \leq 0.1$. We see that for most parameters it follows indeed the prediction from Eq. (S16). However, near $\delta \approx -2J$ the region of validity extends to very low velocities, which can be explained by the qualitative arguments given above. We also see an additional kick at $v/\bar{c} \simeq 0.22$ and $\delta/(2J) = -1$. As shown in Fig. S1 d), in this case also the Ω-sideband hits a divergency in the photonic density of states and therefore induces a significant perturbation.

II. EXACT DYNAMICS FOR AN ATOM MOVING AT THE SPEED OF LIGHT

In this section we derive the exact dynamics of a single atom moving at the maximum speed of light $v = \bar{c}$. As explained in the main text, under this condition there appears a higher order divergence in the co-moving photonic density of states at a frequency $\omega_c = -\pi J$. For the following analytic results we assume $\omega_a \simeq \omega_c$ and approximate the dispersion relation by an infinite cubic band, i.e., $\tilde{\omega}_k \simeq \omega_c - \frac{Ja^3}{3}(k - k_c)^3$, where $k_c = \pi/(2a)$ is the wave vector

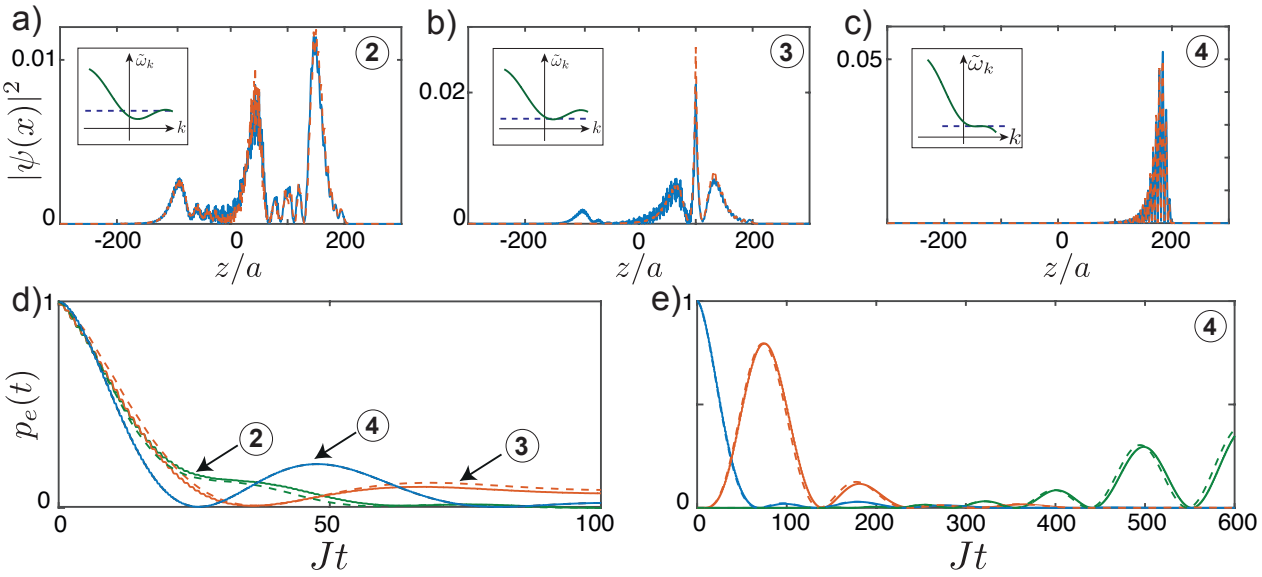

FIG. S2. Comparison of the predictions of the full model (continuous line) and the effective model (dashed line). a)-c) Wave function of the emitted photon evaluated at $t = 100/J$ for the cases: a) $v = \bar{c}/2$ and $\delta/(2J) = -0.5$, b) $v = \bar{c}/2$ and $\delta/(2J) = -1.1$ and c) $v = \bar{c}$ and $\delta/(2J) = -\pi/2$. d) Decay of the excited state population corresponding to the previous cases. e) Excitation transfer between three atoms with $v = \bar{c}$ and $\delta/(2J) = -\pi/2$. In all the plots $g/(2J) = 0.1$ and $z_0/a = 0.1$ is assumed.

corresponding to the frequency ω_c. In the co-moving frame the Hamiltonian for a single atom reads

$$\tilde{H} \simeq \omega_a |e\rangle\langle e| + \int_{-\frac{\pi}{a}}^{\frac{\pi}{a}} dk\, \tilde{\omega}_k a_k^\dagger a_k + \sqrt{\frac{a}{2\pi}} \int_{-\frac{\pi}{a}}^{\frac{\pi}{a}} dk\, \bar{g} \left(e^{ikz_e} a_k \sigma_+ + e^{-ikz_e} a_k^\dagger \sigma_- \right), \tag{S20}$$

where z_e is the initial position of the atom that from now on, without loss of generalization, we will fix to: $z_e = 0$. Having approximated the dispersion as cubic, all the eigenstates of the system are scattering states with eigenvalues in the continuum labelled by the wavevector k, i.e., $E_k = \tilde{\omega}_k$. A generic eigenstate in the single-excitation sector of this Hamiltonian has the form $|\phi_k\rangle = \left[c_e^k \sigma_+ + \int dk'\, \psi_k(k') a_{k'}^\dagger\right]|g\rangle|\text{vac}\rangle$ and by plugging this ansatz into the Schrödinger equation, $\tilde{H}|\phi_k\rangle = E_k|\phi_k\rangle$, we obtain the coupled equations

$$\begin{aligned} c_e^k (E_k - \omega_a) &= \bar{g} \sqrt{\frac{a}{2\pi}} \int dk' \psi_k(k'), \\ \psi_k(k')(E_k - \tilde{\omega}_{k'}) &= \bar{g} \sqrt{\frac{a}{2\pi}}\, c_e^k. \end{aligned} \tag{S21}$$

As previously mentioned the photonic wave function $\psi_k(k')$ is a scattering state thus we need to use the Lippmann-Schwinger equation that in momentum representation reads [S1, S2]

$$\psi_k(k') = \sqrt{\frac{a}{2\pi}} \frac{\bar{g} c_e^k}{\tilde{\omega}_k - \tilde{\omega}_{k'} \pm i\epsilon} + \delta(k - k'), \tag{S22}$$

where we used $E_k = \tilde{\omega}_k$. In this way is possible to write the atomic amplitude as

$$c_e^k = \bar{g} \sqrt{\frac{a}{2\pi}} \frac{1}{\tilde{\omega}_k - \bar{\delta} - \bar{g}^2 I_0(\tilde{\omega}_k)}, \tag{S23}$$

where the integral $I_z(\tilde{\omega}_k)$ is defined as

$$\begin{aligned} I_z(\tilde{\omega}_k) = \sqrt{\frac{a}{2\pi}} \int dk' \frac{e^{ik'z}}{\tilde{\omega}_k - \tilde{\omega}_{k'} \pm i\epsilon} = &- \frac{\text{sgn}[k - k_c] e^{-i\frac{\pi}{6}\text{sgn}[(k-k_c)z]}}{Ja^2(k - k_c)^2} \\ &\times \left(e^{i\frac{(k-k_c)z}{2} - \frac{\sqrt{3}}{2}|(k-k_c)z|} + e^{i\frac{2}{3}\pi \text{sgn}[(k-k_c)z] - i(k-k_c)z} \right), \end{aligned} \tag{S24}$$

where sgn(k) is the sign function. In the evaluation of the previous integral was taken the limit $\epsilon \to 0$ assuming $+\epsilon$ for $z > 0$ and $-\epsilon$ for $z < 0$ in order to have a convergent result. The generic eigenstate can be written in momentum space as

$$|\phi_k\rangle = \left[c_e^k \sigma_+ + a_k^\dagger + \sqrt{\frac{a}{2\pi}} \int dk' \frac{\bar{g} c_e^k}{\tilde{\omega}_k - \tilde{\omega}_{k'}} a_{k'}^\dagger\right] |g\rangle|\text{vac}\rangle. \tag{S25}$$

In real space the eigenstates read

$$|\phi_k\rangle = \left[c_e^k \sigma_+ + \int dx\, \psi_k(z) a_z^\dagger\right] |g\rangle|\text{vac}\rangle, \tag{S26}$$

where the atomic and photonic amplitudes are given by

$$\psi_k(z) = \frac{1}{\sqrt{2\pi}} \left[e^{-ikz} + \gamma_{kz} \left(e^{i\frac{(k-k_c)z}{2} - \frac{\sqrt{3}}{2}|(k-k_c)z|} + e^{i\frac{2}{3}\pi \text{sgn}[(k-k_c)z] - i(k-k_c)z}\right)\right], \tag{S27}$$

$$c_e^k = \frac{\bar{g}}{\sqrt{2\pi}} \frac{Ja^2(k-k_c)^2}{(\tilde{\omega}_k - \bar{\delta})Ja^2(k-k_c)^2 + \bar{g}^2 \text{sgn}(k-k_c) e^{-i\frac{\pi}{6}\text{sgn}[(k-k_c)z]} \left[1 + e^{i\frac{2}{3}\pi \text{sgn}[(k-k_c)z]}\right]}, \tag{S28}$$

$$\gamma_{kz} = \frac{-\bar{g}^2 \text{sgn}(k-k_c) e^{-i\frac{\pi}{6}\text{sgn}[(k-k_c)z]}}{(\tilde{\omega}_k - \bar{\delta})Ja^2(k-k_c)^2 + \bar{g}^2 \text{sgn}(k-k_c) e^{-i\frac{\pi}{6}\text{sgn}[(k-k_c)z]} \left[1 + e^{i\frac{2}{3}\pi \text{sgn}[(k-k_c)z]}\right]}. \tag{S29}$$

The derivation of the eigenstates for multiple atoms can be obtained similarly.

Using these exact solutions we can investigate the spontaneous emission of an initially excited atom. The time evolution of the atom-field dressed state $|\psi(t)\rangle$ can be expressed in terms of the eigenstates of the system according to

$$|\psi(t)\rangle = \int dk\, c_e^{k*} e^{-i\tilde{\omega}_k t} |\phi_k\rangle. \tag{S30}$$

From that is possible evaluate the emitted photonic wave packet shown in Fig. 2 d) of the main text,

$$\psi(z,t) = \langle z|\psi(t)\rangle = \int dk\, \psi_k(z) c_e^{k*} e^{-i\tilde{\omega}_k t}. \tag{S31}$$

The probability of finding the atom in the excited state as function of time can also be computed by evaluating $p_e(t) = |\langle e|\psi(t)\rangle|^2$ and is given by the following expression

$$p_e(t) = \left| \frac{\eta^2}{2\pi} \int dq \frac{q^4 e^{i\frac{q^3 \bar{t}}{6}}}{[\frac{q^5}{3} - \text{sgn}(q)\eta^2 \frac{\sqrt{3}}{2}]^2 + \frac{\eta^4}{4}} \right|^2, \tag{S32}$$

where the dimensionless parameters $\eta = \bar{g}/J$, $q = ka$ and $\bar{t} = 2Jt$ were introduced. To obtain a simpler approximate result we can instead consider the Laplace transform of the atomic amplitude

$$c_e(s) = \frac{1}{s + i\bar{\delta} + \bar{g}^2 I(s)}, \tag{S33}$$

where

$$I(s) = -i\frac{a}{2\pi} \int dk \frac{1}{\tilde{\omega}_k - is} = (9Js^2)^{-1/3}. \tag{S34}$$

By assuming to be exactly on resonance with the flat part of the band, $\bar{\delta} = 0$, we can rewrite $c_e(s)$ as

$$c_e(s) = \frac{1}{s + i\bar{g}\left(\frac{s}{9J}\right)^{1/6}} + \frac{1}{s - i\bar{g}\left(\frac{s}{9J}\right)^{1/6}} \simeq \frac{1}{s + i\Omega_c + \Gamma_c/2} + \frac{1}{s - i\Omega_c + \Gamma_c/2}, \tag{S35}$$

where in the last we made a single pole approximation. Under this approximation the inverse Laplace transform of $c_e(s)$ results in a damped cosine function as given in Eq. (4) of the main text. The coefficients

$$\Omega_c = \frac{\sqrt{5+\sqrt{5}}}{2\sqrt{2}} \left(\frac{g^6}{9J}\right)^{1/5}, \qquad \Gamma_c = \frac{\sqrt{5}-1}{2} \left(\frac{g^6}{9J}\right)^{1/5}, \tag{S36}$$

represent the characteristic oscillation frequency and the damping rate, respectively.

III. ESTIMATE OF THE ATOM-FIELD COUPLING STRENGTH FOR CPW RESONATORS

In the main text we describe the implement of a slow-light waveguide QED system using Rydberg atoms flying above a superconducting coplanar waveguide (CPW) resonator array [S3]. The geometry of the resonator is shown in Fig. (4) of the main text. For a transition dipole moment $d = n^2 a_0 e$ (where a_0 is the Bohr radius) between two neighboring Rydberg levels $|n\rangle$ and $|n+1\rangle$, the atom-field coupling strength is

$$g = \frac{d}{\hbar}|\vec{E}(x,y,z)|, \tag{S37}$$

where $\vec{E}(x,y,z)$ is the electric field of the resonator mode per photon. In a quasi 1D waveguide resonator the electric field is of the form

$$\vec{E}(x,y,z) = [E_z(z,y)\vec{e}_z + E_y(z,y)\vec{e}_y]\cos\left(\frac{m\pi x}{L_x}\right), \tag{S38}$$

where L_x is the length of the resonator and the same coordinate as in Fig. 4 in the main text have been assumed.

To estimate the transverse electric field profile we consider the limit of an infinitely flat CPW resonator of length L_x and an additional ground plate located at a distance h below the central track. According to Ref. [S4], if the width of the two external ground planes is bigger than twice the gap between them, they can be treated as infinitely extended. With this assumption, an exact solution for the electric field above the central electrode of the CPW resonator can be obtained using conformal mapping technics [S5]. In particular, the two transversal field component are given by $E_z(z,y) = \mathrm{Im}\{E(t)\}$ and $E_y(z,y) = \mathrm{Re}\{E(t)\}$, where

$$E(t) = \begin{cases} \frac{E_0}{\sqrt{(\frac{t^2}{l_1^2}-1)(\frac{t^2}{l_2^2}-1)}} & y > 0 \\ \frac{E_0}{\sqrt{(\cosh^2\frac{\pi t}{2h}-\cosh^2\frac{\pi l_1}{2h})(\cosh^2\frac{\pi t}{2h}-\cosh^2\frac{\pi l_2}{2h})}} & -h < y < 0 \end{cases} \tag{S39}$$

with $t = z + iy$ and l_1, l_2 related to the size of the middle electrode and to the ground planes separation [see Fig. 4b) in the main text]. In the previous expression we introduced the electric field per photon, $E_0 = \sqrt{\frac{\hbar\omega}{\epsilon_0 V_r}}$, where ϵ_0 is the vacuum dielectric constant and V_r the mode volume of the resonator given by

$$V_r = \frac{L_x}{2}\left[\int_{-\infty}^{\infty} dz \int_{-h}^{\infty} dy \left(E_z^2(z,y) + E_y^2(z,y)\right)\right]. \tag{S40}$$

For the parameters considered in the main text and $h < 5\mu$m, the volume below the central electrode is negligible compare to the mode volume above and only the latter must be considered for the evaluation of the field strength E_0.

IV. DISORDER

Periodic photonic structures are usually subject to imperfections and disorder in the lattice fabrication. This results in random frequency offset between neighboring lattice sites, which in turn can lead to localization. We can model the effect of such disorder by adding a random frequency offset $\delta\omega_\ell$ for each local resonator mode, i.e., $H_{\mathrm{dis}} = \sum_{\ell=1}^{N_L} \delta\omega_\ell a_\ell^\dagger a_\ell$. In momentum space this corresponds to the Hamiltonian

$$H_{\mathrm{dis}} = \sum_{k,k'} f_{k,k'} a_k^\dagger a_{k'}, \tag{S41}$$

where $f_{k,k'} = \frac{1}{N_L}\sum_\ell e^{i(k-k')\ell}\delta\omega_\ell$. For numerical simulations we chose the $\delta\omega_\ell$ randomly from a uniform distribution in the interval $[-\epsilon/2, \epsilon/2]$.

In Fig. S3 a) and b) we plot the atomic population and the wave function of the emitted photon for the case $v/\bar{c} = 0.5$ and $\delta/(2J) = -0.5$ and for different values of the disorder strength ϵ. From the plots we see that the system dynamics is almost unaffected by the disorder up to values of about $\epsilon/(2J) = 0.1$. Above this value the signatures of a co-moving bound state are washed out. In Fig. S3 c) and d) we plot the analog results for the critical coupling conditions $v/\bar{c} = 1$ and $\delta/(2J) = -\pi/2$. Here we find that the atomic decay is even less affected by disorder. However,

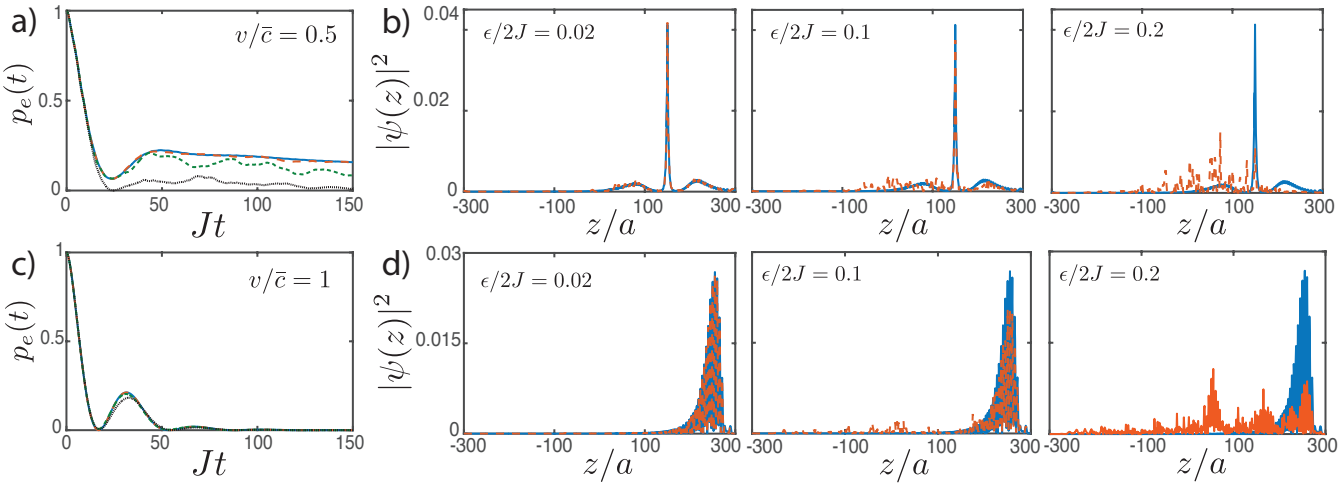

FIG. S3. Effects of disorder for the cases $v/\bar{c} = 0.5$, $\delta/2J = -0.5$ a)-b) and $v/\bar{c} = 1$, $\delta/2J = -\pi/2$ c)-d). In picture a)-c) is shown the excited state population for the cases $\epsilon/2J = 0$ (continuous line), $\epsilon/2J = 0.02$ (long dashed), $\epsilon/2J = 0.1$ (small dashed) and $\epsilon/2J = 0.2$ (dotted). In picture b)-d) are shown the comparison of the emitted photon wavepackets (evaluated at $t = 110/J$) for the cases with (dashed) and without disorder (continuous). In all the plot is assumed $\bar{g}/(2J) = 0.1$.

for $\epsilon/(2J) > 0.1$ the emitted wavefunction is becomes again significantly distorted, which would affect the dynamics of excitation transfer processes.

In conclusion, we find that all the effects described in the main text are robust with respect to disorder up to a strength of the order of $\epsilon/(2J) \simeq 0.1$. In the CPW resonators array implementation this would corresponds a variation in the frequency of each resonator of about $\epsilon \simeq 0.8$ MHz. This accuracy is achievable with the state of the art fabrication technology [S8]. For further discussions on the effect of disorder in coupled resonator waveguides see also Ref. [S6] and the supplementary material of [S7].

[S1] F. Lombardo, F. Ciccarello, and G. M. Palma, *Photon localization versus population trapping in a coupled-cavity array*, Phys. Rev. A **89**, 053826 (2014).
[S2] E. N. Economou, *Green Functions in Quantum Physics* (Springer-Verlag, Berlin, 1979).
[S3] D. Petrosyan and M. Fleischhauer, Phys. Rev. Lett. **100**, 70501 (2008).
[S4] G. E. Ponchak, E. M. Tentzeris, and L. P. B. Katehi, Int. J. Microcircuits Electronic Packaging **20**, 2 (1997).
[S5] M. Gillick, I. D. Robertson, and J. S. Joshi, IEEE Trans. Microw. Theory Tech. **41**, 1 (1993).
[S6] S. Lorenzo, F. Lombardo F. Ciccarello, and G. M. Palma, arXiv:1609.04158v1 (2016).
[S7] J. S. Douglas, H. Habibian, C. L. Hung, A. V. Gorshkov, H. J. Kimble, and D. E. Chang, Nature Photon. **9**, 326 (2015).
[S8] D. Underwood, W. E. Shanks, J. Koch, and A. A. Houck, *Low disorder microwave cavity lattices for quantum simulation with photons*, Phys. Rev. A **86**, 023837 (2012).